The International Journal of Advanced Manufacturing Technology (2019) 105:1637–1644
https://doi.org/10.1007/s00170-019-04368-9

ORIGINAL ARTICLE

The effect of PSD on properties of unimodal and bimodal powders using 17-4 PH stainless steel powder

N. S. Muchavi[1] · M. Seerane[1] · R. Machaka[1,2]

Received: 20 June 2019 / Revised: 23 August 2019 / Accepted: 27 August 2019 / Published online: 14 October 2019

Abstract

17-4 PH is a martensitic precipitation-hardening stainless steel that possesses an outstanding combination of superior physical and mechanical properties, good toughness, resistance to corrosion, and is easily machinable and weldable. It is widely used in the chemical, petrochemical, and aerospace industries. In this paper, we study the effect of the particle size distribution of unimodal and bimodal powders on properties of 17-4 PH stainless steel parts manufactured through metal injection molding (MIM). Unimodal and bimodal injectable MIM feedstocks of 60 vol% solids loading were prepared using powders of three different particle sizes with a wax-based binder system. The results show that coarser particle sizes (unimodal or bimodal) exhibit relatively lower shrinkage levels which is desirable for dimensional control but inferior "as-sintered" mechanical properties. The finer particle sizes (unimodal or bimodal) exhibited inferior rheological feedstock properties but comparatively superior "as-sintered" mechanical properties. The study suggests that bimodal feedstocks of finer particle sizes exhibit a favorable combination of rheological properties and "as-sintered" mechanical properties.

Keywords Metal injection molding · Particle size · 17-4 PH stainless steel · Bimodal feedstocks · Mechanical properties

1 Introduction

Numerous researchers have reported on attempts to fabricate 17-4 PH stainless steel components via powder metallurgy techniques [1–5]. Challenges associated with fabricating 17-4 PH components with desired properties via powder metallurgy processes such as the conventional press and sinter (PS) and additive manufacturing (AM) techniques have been documented [2, 5–7]. These challenges include low powder compressibility for PS [4, 6] and the undue residual stress accumulation from martensitic transformation during deposition for AM [2, 5, 7]. More recent reports have however widely reported on the attractiveness of metal injection molding (MIM) in the fabrication of complex, near-net shaped 17-4 PH stainless steel components. For example, Wu et al. have reported MIM of 17-4 PH stainless steel and the results showed that better mechanical properties of this alloy can be achieved through MIM [8].

MIM is an attractive powder metallurgy technique that, in recent years, has developed to be a cost-effective manufacturing process for high-volume production of intricately shaped parts where high-dimensional accuracy is required [9–11]. It is a multistep process by its nature; involving the preparation of suitable feedstocks, injection molding, solvent/catalytic and thermal debinding, high-temperature sintering, and post-sintering processing if required. The mechanical properties of final MIM components are highly dependent on several factors such as the starting powder material and feedstock characteristics, as well as the fabrication process itself [12]. Even though the effects of the starting powder

✉ R. Machaka
rmachaka@csir.co.za

N. S. Muchavi
nmuchavi@csir.co.za

M. Seerane
mseerane@csir.co.za

[1] Advanced Manufacturing & Engineering, Manufacturing Cluster, Council for Scientific and Industrial Research, 627 Meiring Naudé Road, Brummeria, Pretoria 0185, South Africa

[2] Department of Metallurgy, School of Mining, Metallurgy and Chemical Engineering, University of Johannesburg, Pretoria 0001, South Africa

material characteristics and MIM processing (viz. debinding and sintering) on the final mechanical properties of 17-4 PH stainless steel parts are well understood [13–19], the effects of feedstock flow stability, on the other hand, appear to not be equally documented.

This can be attributed to the existence of numerous and seemingly unrelated rheological parameters where each parameter often gives incomplete or conflicting insights into the formulated feedstocks' qualities [20, 21]. For this study, two general parameters are sought—the feedstock flow stability and the moldability index (α_{stv}). The feedstock flow stability measures the consistency of the viscosity. The moldability index is a more generalized parameter commonly used as a comparative indicator of feedstock qualities (superiority/inferiority) with respect to its rheological behavior and moldability characteristics [21–25]. The moldability index exists in the literature in various forms, for this work, it is defined as in Eq. (1) below after the Weir model of polymers [26]:

$$\alpha_{stv} = \frac{1}{\eta_0}\frac{1-n}{\left(E/R\right)} \tag{1}$$

where the subscripts s, t, and v represent the index's sensitivity to the shear rate, temperature, and viscosity variations, respectively, whereas η_0, n, E, and R indicate viscosity at a reference temperature, power-law flow index behavior, activation energy for the Arrhenius temperature dependence of the viscosity, and the gas constant, respectively [20, 21, 23, 24].

Our preliminary studies investigated on the effect of powder particle size on mechanical the properties of 17-4 PH stainless steel (using the – 5-, − 15-, and – 45-μm unimodal feedstocks) demonstrated that the sintered − 5-μm feedstock achieved the highest final density as well as superior moldability during injection molding [12]. Further studies on the rheological properties of 17-4 PH stainless steel MIM feedstocks concluded that at high shear rates, feedstocks of bimodal powder distributions exhibit higher moldability index values which exemplify better rheological behavior during injection molding [27]. This current report is intended to evaluate the influence of the feedstock moldability index and flow stability of bimodal MIM feedstocks on the physical and mechanical properties of as-sintered 17-4 PH stainless steel.

2 Materials and experimental methods

Figure 1 shows the scanning electron micrographs of the unimodal − 5-μm, − 15-μm, and – 45-μm 17-4 PH stainless steel powder materials used for this study. The – 5-μm and – 15-μm powder materials were supplied by Epson Atmix Corporation (JP) and the – 45-μm powder material by Praxair Surface Technologies.

Using a proprietary polymer wax–based binder system and the said powder materials, five 60 vol% ready-to-inject feedstocks were formulated; a summary of the feedstocks is shown in Table 1. The 25:75 bimodal powder blending follows Joo Won Oh [28].

The feedstock rheology was characterized using a Ceast SmartRheo capillary rheometer (Pianezza TO, Italy). The capillary used has a length-to-diameter ratio of 5:1 and shear rates ranging from 1000 to 10,000 s^{-1} were applied. All prepared feedstocks were tested at 110, 120, 130, and 140 °C as reported prior in reference [27].

The molding of the "dog-bone" tensile specimen, specified according to the ISO 2740 standard, at prior determined optimum injection molding parameters given in Table 2. The dimensions of the dog-bone tensile specimens were 88 mm (overall length), 40 mm (gauge length), 14.8 mm (grip section diameter), and 5 mm (gauge section diameter), see Fig. 2. Debinding of green specimens was achieved in two steps—first in *n*-heptane (Merck Millipore) at 60 °C for 24 h and thermally at 600 °C for 1 h in a Carbolite tube furnace. A pre-sintering step of the brown specimens was carried out at 1000 °C for 1 h in a Carbolite tube furnace under an argon gas flowing (at 1.0 L/min) environment.

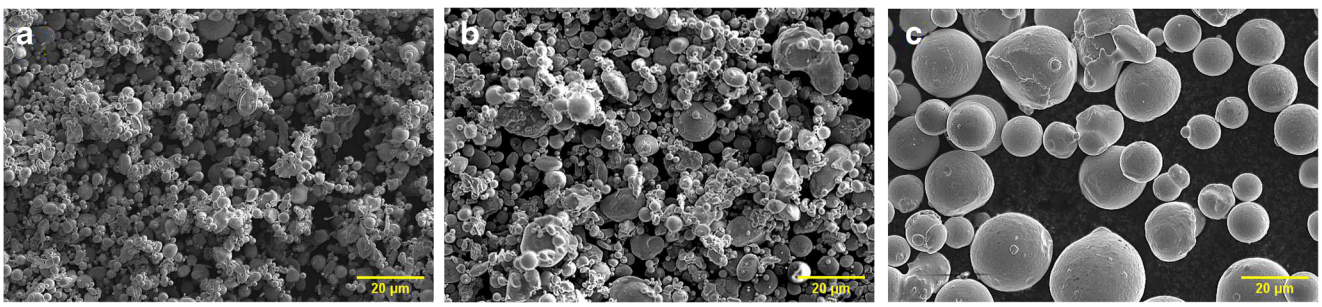

Fig. 1 Scanning electron micrograph (SEM) of – 5-μm (**a**), − 15-μm (**b**), and – 45-μm (**c**) 17-4 PH stainless steel powder. Adapted from [27], with permission

Table 1 Feedstock formulations used in this study

Feedstock ID	Feedstock information
PS-5	60 vol%; powder, − 5 μm
PS-15/5	60 vol%; powder, 75% − 15 μm + 25% − 5 μm
PS-15	60 vol%; powder, − 15 μm
PS-45/15	60 vol%; powder, 75% − 45 μm + 25% − 15 μm
PS-45	60 vol%; powder, − 45 μm

Sintering was performed at temperatures of up to 1300 °C at 10 °C/min for 3 h in a Xerion vacuum furnace. Sintered samples were evaluated for shrinkage, apparent density, microstructure, pore sizes and distribution, hardness, and tensile properties. The densities were evaluated using a precision analytical balance (OHAUS) based on the Archimedes' technique according to ASTM B962-08 and Spierings et.al [30, 31].

A Leica DMI500 M optical microscope was used to observe the as-sintered microstructures. Apparent hardness measurements were carried using a Vickers microhardness tester (FM-700) with a 500 g load applied for 10 s as per ASTM-E384 standard. Tensile testing was done on an instrumented INSTRON™ Servo Hydraulic 1342 test apparatus at a strain rate of 0.5 mm/min. The linear shrinkages of the sintered samples were measured against the as-molded green parts using a Vernier caliper.

Figure 2 illustrates the visual differences between the as-molded, solvent debound, and sintered (PS-45/5 for example) specimens. The appearance of specimens in Fig. 3 indicates the level of shrinkage that occurred during processing. Specimen (b) underwent solvent debinding and no shrinkage difference is observed relative to the as-molded part, whereas, specimen (c) underwent sintering and shows remarkable shrinkage relative to the as-molded part.

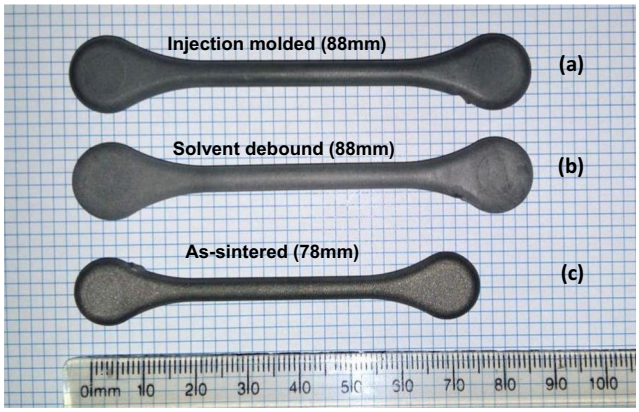

Fig. 2 Shrinkage variations in the specimens at 60 vol%. **a** As-molded. **b** Solvent debound. **c** As-sintered

3 Results and discussion

3.1 Rheological properties

The results presented in this section endeavor to extend the findings from our previous studies by exploring the influence of the feedstock flow stability and moldability index parameters on the mechanical properties of the MIM materials produced from the feedstocks studied prior.

Table 2 Optimum injection molding parameters [29]

Process parameter	Optimum conditions
Nozzle temperature	140–160 °C
Barrel temperature	120–140 °C
Mold temperature	30–40 °C
Injection pressure	800–900 bars
Injection speed	4.5 ccm/s
Cooling time	5 s
Holding pressure	800 bars

Adapted from reference [29]

Figure 3 summarizes the findings from a recent report on the effects of the powder size distribution on numerous rheological properties of 17-4 PH stainless steel MIM feedstocks [27]. Figure 3 a shows the variation of the measured viscosity of the feedstocks with the shear rate at the minimum injection temperature. Figure 3 b shows the effects of bimodal powder distributions on feedstock stability (flow activation energy) and moldability index.

Subdued variations of the measured viscosity of the feedstocks are an indication of the "stability." Feedstock instability has been attributed to the size-segregation of powder particles and local loading variations in the feedstock during flow [32, 33]. Bimodal feedstocks and agglomerated fine powder-based feedstocks exhibited apparent flow instability, especially at lower shear rates. According to Khakbiz et al. [34], at relatively low shear rates, such feedstocks instability tentatively manifest small density or pore distribution variations, especially in the bimodal feedstocks. However, the results show that the feedstocks become stable at higher shear rates (typical injection molding conditions) as the breakup of agglomerates and clusters lead to increased particle-particle interaction to aid flow in accordance [35].

Higher moldability index (α_{stv}) values infer superior rheological properties and desirable moldability qualities [22, 24]. Figure 3 b indicates that the FS-15 and FS-5/15 MIM feedstocks give significantly high moldability index values at high shear rates, where the injection molding is intended. The feedstocks formulated from the coarser powder (FS-45 and FS-15/45 in this case) consistently exhibit inferior moldability along with the FS-5 unimodal feedstock.

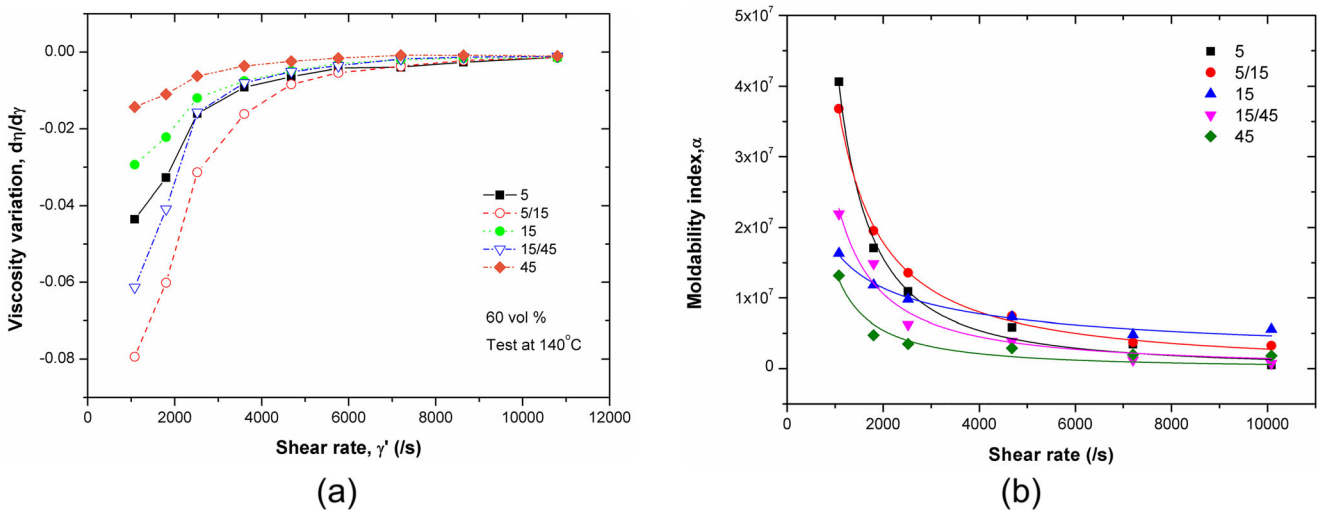

Fig. 3 **a**, **b** A summary of the rheological properties of feedstocks tested. From [27], with permission

Particle size analysis and the SEM micrographs of the starting powders − 5 μm, as seen in Fig. 1a, exhibit a considerable degree of agglomeration compared with the coarser − 45-μm powder material seen in Fig. 1c. Particle size analysis and the SEM micrograph of the − 15 μm powder materials shows a hint of a multimodal distribution.

According to references [16, 23, 36–38], at high shear rates, the FS-15 and FS-5/15 feedstocks could be ideal for MIM requiring very complex geometries/features or microMIM.

3.2 Microstructure and physical properties

The optical micrographs demonstrating the resulting microstructures of the sintered specimens are shown in Fig. 4a–e while Fig. 4 f shows the image analysis of the representative micrographs of the sintered feedstocks as exhibited in Fig 4a–e. The relative density and shrinkage behavior of the sintered materials are displayed in Fig. 5.

The coarse PS-45 and fine PS-5 unimodal feedstocks as well as the PS-45/15 bimodal-based feedstocks demonstrated lower sintered densities. The lower sintered densities in the PS-45 unimodal and PS-45/15 bimodal feedstocks can easily be attributed to the fact that larger particles tend to have lower sintering rates thus less shrinkage [38–40]. As a testament, the pore size distributions obtained by image analysis of the micrographs also show abundant, relatively larger, and characteristically irregular pore structures. On the other hand, the low densities in the PS-5 unimodal feedstock can be attributed to the inefficient particle packing associated with agglomeration and fine powder surface chemistry [39, 41]. The PS-5 unimodal feedstock possibly shows the most shrinkage which indicates that the powder had a lower starting packing density.

Conversely, the as-sintered PS-5 and PS-P15 microstructures exhibit relatively uniformly distributed fine and spherical pore structures—an indication that the finer starting powder materials resulted in comparatively better sinterability (compared with the relatively coarse unimodal feedstocks). Prior reports by Kearns and co-workers [40] further collaborate with this observation.

Generally, higher porosity is expected in conventional PM parts (when compared with wrought materials) [1, 42]. However, if MIM is to find industrial applications, MIM parts are expected to be “fully dense and comparable in properties with their wrought equivalents” [43]. In this work, perhaps one of the most significant differences between the micrographs of the unimodal and bimodal as-sintered materials lies in the density and distribution of pores as exhibited in Fig. 4f. Finer starting powder particle sizes, in general, result in finer pores. In addition, and as also demonstrated in computer simulations and in practice [18, 38, 39, 44], improving gap-filling and the propensity for particle rearrangement in the bimodal feedstocks typically leads to improved sinterability and even finer and narrower pore distributions as well as enhanced mechanical properties.

Feedstocks that exhibit superior rheological behavior of significantly higher moldability index values in Fig. 3b, i.e., formulated using the – 15 and 5/15-μm powder, yielded favorable densification [28] and more uniform sintered microstructures in the case of the 5/15-μm powder. The as-sintered densities are comparable with the minimum specifications for 17-4 PH MIM materials as specified by various suppliers (powder and MIM feedstock), as according to prior studies available in the literature and the respective Metal Powder Industries

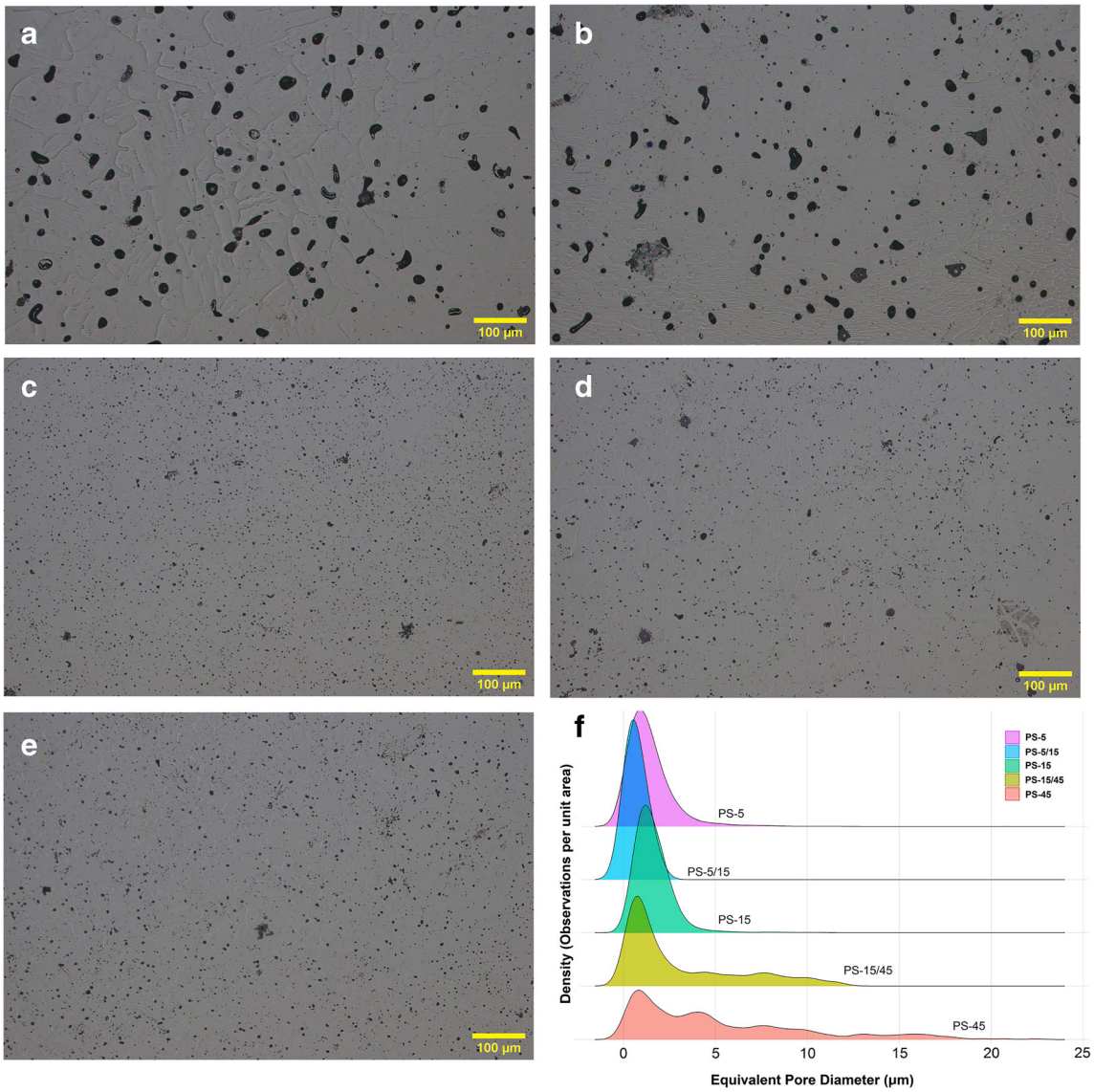

Fig. 4 Optical micrographs showing the microstructures of the sintered materials, i.e., PS-45 (**a**), PS-45/15 (**b**), PS-15 (**c**), PS-15/5 (**d**), and PS-5 (**e**). **f** Representative pore size distributions obtained by image analysis of the micrographs (shown in Fig. 3(**a**–**e**))

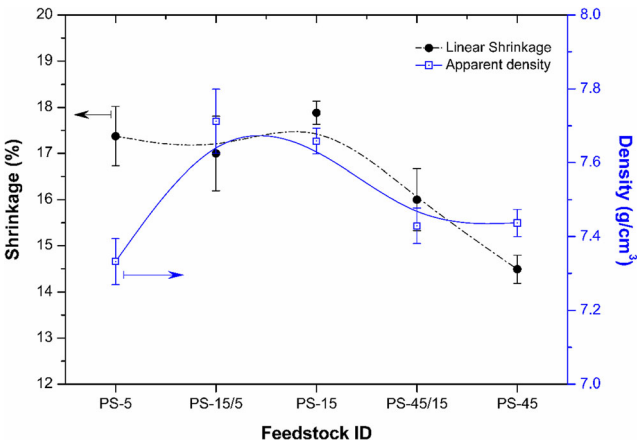

Fig. 5 Representation of the shrinkage and densification behavior of the feedstocks

Federation (MPIF) and American Society for Testing and Materials (ASTM) standards [45, 46].

3.3 Mechanical properties

Table 3 gives a summary of the "as-sintered" mechanical properties of the test samples used in this study. Tensile properties generally improve with bimodal powder distributions. This observation can be attributed to the increasing densification and grain boundary volume as the particles become finer [28, 39]. Tang and Pistorius [47] indicated that defects including porosity control fatigue life. Fotovvati et al. [48] summarized these defects as residual stresses, surface roughness, internal defects, and microstructural inhomogeneities. These defects are typically the origin of fatigue cracks; thus,

Table 3 Properties of as-sintered parts 17-4 PH stainless steel against MPIF standards

Feedstock	App. density (g/cm^3)	YS (MPa)	UTS (MPa)	Elongation (%)	Hardness (HV)
FS-5	7.34 ± 0.06	743	1140	5	379 ± 2.1
FS-15/5	7.72 ± 0.09	714	890	8	315 ± 7.3
FS-15	7.66 ± 0.03	765	772	2	267 ± 3.5
FS-45/15	7.43 ± 0.05	648	806	6	225 ± 8.9
FS-45	7.44 ± 0.04	700	719	4	228 ± 9.6
MPIF standard[†]	7.50	650	790	4	279

[†] The Metal Powder Industries Federation (MPIF) Standard 35 for MIM Products provides the standardized material designation code, chemical composition specifications, the minimum acceptable engineering property data (in both inch-pound and SI units), and other relevant information to specify materials for MIM-fabricated parts. MPIF is a "not-for-profit" association formed by the metal powder producing and consuming industry associations in order to promote the development of essential standards and testing methods

abundantly larger irregular pores are subject to acting as crack initiation sites and therefore reducing fatigue life. Fatigue and tensile behaviors are monotonic; hence, poor tensile properties of feedstocks FS-45 and FS-45/15 are a direct indication of inferior fatigue life of the samples and this is attributed to larger porosity (Fig. 4 a and b). Even though the PS-5 sintered material exhibited desirable tensile strength and ductility and hardness properties, the occurrence of fine pore structures appears to have led to sintered densities below the minimum specifications for 17-4 PH MIM products.

As-sintered mechanical properties of 17-4 PH stainless steel products are largely determined by microstructures, including the porosity. This is supported by Gülsoy, Özbek, and Baykara [1], Kearns and co-workers [40], and German [49]. The bimodal feedstocks, and PS-15/5 in particular, exhibit the best combination of low cumulative pore volumes and mechanical properties exceeding the minimum property values as set-out in the MPIF Standard 35 for MIM products [49]. By observation, SEM micrograph of the − 15-μm powder appears bimodally distributed, see Fig. 1a.

Superior rheological properties of feedstocks generally lead to favorable as-sintered mechanical properties. Significantly higher moldability indices, for the − 15 and 5/15-μm feedstocks in particular, possibly indicated the breakup of powder agglomerates and clusters to aid flow [35] and also lead to increased densification and grain boundary volume as the particles become finer [28, 39]. The same argument holds when the as-sintered mechanical properties of the FS-45/15 bimodal feedstock are compared with that of the FS-45 feedstock.

4 Conclusions

This current report is an extension of prior published work. This work has evaluated the influence of the feedstock moldability index and flow stability of bimodal MIM feedstocks on the physical and mechanical properties of as-sintered 17-4 PH stainless steel materials.

A review of the rheological properties of 17-4 PH stainless steel MIM feedstocks and the physical and mechanical properties of as-sintered 17-4 PH stainless steel materials were presented.

The results show that coarser particle sizes (unimodal or bimodal) exhibited relatively lower shrinkage levels which is desirable for dimensional control but inferior "as-sintered" mechanical properties (viz. tensile and fatigue behavior). While the finest unimodal feedstock used in this work exhibited inferior rheological feedstock properties and mechanical properties, bimodal feedstocks formulations exhibited higher moldability index values which exemplify better rheological behavior during injection molding [27] and comparatively improved as-sintered mechanical properties. Tentatively, a higher feedstock moldability index is an indicator of favorable as-sintered mechanical properties.

Acknowledgments Epson Atmix Corporation in Japan is thanked for the supply of the powders used in this study. The contributions of *Ntate* Sam Papo, Lusanda Fikeni, Ntswaki Nyakane, Filipe Pereira, Chris McDuling, and Pierre Rossouw are duly recognized. We are also truly indebted to Phumlani Ndlangamandla, who collected some of the results as an undergraduate student from the University of Pretoria so as to his supervisor Vinod Kurup.

Author contributions Study conception and design: Ronald Machaka (RM) and Phumlani Ndlangamandla (PN); Acquisition and processing of experimental data: Noluntu S. Muchavi (NSM), PN, RM, Mandy Seerane (MS), Lusanda Fikeni (LF), and Ntswaki Nyakane (NN); Analysis and interpretation of data: NSM, MS, and RM; Drafting of the manuscript: NSM, MS, and RM; Critical revision: NSM, MS, and RM; Final approval: NSM, MS, and RM; Lead and guarantor author: RM

Funding information The CSIR supported this work through a Parliamentary Grant and the Department of Science and Innovation also supported this work through the Advanced Material initiative.

References

1. Gülsoy HÖ, Özbek S, Baykara T (2007) Microstructural and mechanical properties of injection moulded gas and water atomised

17-4 PH stainless steel powder. Powder Metall 50:120–126. https://doi.org/10.1179/174329007X153288
2. Murr LE, Gaytan SM, Ramirez DA, Martinez E, Hernandez J, Amato KN, Shindo PW, Medina FR, Wicker RB (2012) Metal fabrication by additive manufacturing using laser and electron beam melting technologies. J Mater Sci Technol 28:1–14. https://doi.org/10.1016/S1005-0302(12)60016-4
3. Kumar VA, Gupta RK, Karthikeyan MK, Prasad KN, Sinha PP, Rao MN, 2007 Processing and characterization of thin sheets of 17-4PH stainless steel for aerospace application, in: Int Conf Adv Mater Compos
4. Neilan A, Warzel III R, Hu B, Neyman R, Hinchliffe J, (2017) Characterization of martensitic stainless steels in PM components, in: Int. Conf. Powder Metall. Part. Mater. (POWDERMET 2017), Metal Powder Industries Federation (MPIF), Las Vegas, USA
5. Murr LE, Martinez E, Hernandez J, Collins S, Amato KN, Gaytan SM, Shindo PW (2012) Microstructures and properties of 17-4 PH stainless steel fabricated by selective laser melting. J Mater Res Technol 1:167–177. https://doi.org/10.1016/S2238-7854(12)70029-7
6. Reinshagen JH, Witsberger JC (1994) Properties of precipitation hardening stainless steel processed by conventional powder metallurgy techniques. Adv Powder Metall Part Mater 7:313–323
7. DebRoy T, Wei HL, Zuback JS, Mukherjee T, Elmer JW, Milewski JO, Beese AM, Wilson-Heid A, De A, Zhang W (2018) Additive manufacturing of metallic components – process, structure and properties. Prog Mater Sci 92:112–224. https://doi.org/10.1016/j.pmatsci.2017.10.001
8. Wu M-W, Huang Z-K, Tseng C-F, Hwang K-S (2015) Microstructures, mechanical properties, and fracture behaviors of metal-injection molded 17-4PH stainless steel. Met Mater Int 21:531–537. https://doi.org/10.1007/s12540-015-4369-y
9. Ferri OM, Ebel T, Bormann R (2010) Influence of surface quality and porosity on fatigue behaviour of Ti–6Al–4V components processed by MIM. Mater Sci Eng A 527:1800–1805. https://doi.org/10.1016/j.msea.2009.11.007
10. Barriere T, Liu B, Gelin JC (2003) Determination of the optimal process parameters in metal injection molding from experiments and numerical modeling. J Mater Process Technol 143–144:636–644. https://doi.org/10.1016/S0924-0136(03)00473-4
11. Pachauri P, Hamiuddin M (2015) Optimization of injection moulding process parameters in MIM for impact toughness of sintered parts. Cloud Publ Int J Adv Mater Metall Eng 1:1–11
12. Seerane M, Ndlangamandla P, Machaka R (2016) The influence of particle size distribution on the properties of metal- injection-moulded 17-4 PH stainless steel. J South Afr Inst Min Metall 116:1–6
13. Chen X, (1998) Particle packing, compaction and sintering in powder metallurgy, University of Alberta
14. Sotomayor ME, Várez A, Levenfeld B (2010) Influence of powder particle size distribution on rheological properties of 316L powder injection moulding feedstocks. Powder Technol 200:30–36. https://doi.org/10.1016/j.powtec.2010.02.003
15. Amin SYM, Jamaludin KR, Muhamad N, (2008) Rheological properties of SS316L MIM feedstock prepared with different particle sizes and powder loadings, 59–63
16. Li Y, Li L, Khalil KA (2007) Effect of powder loading on metal injection molding stainless steels. J Mater Process Technol 183:432–439. https://doi.org/10.1016/j.jmatprotec.2006.10.039
17. Zheng J, Carlson WB, Reed JS (1995) The packing density of binary powder mixtures. J Eur Ceram Soc 15:479–483. https://doi.org/10.1016/0955-2219(95)00001-B
18. German RM (1992) Prediction of sintered density for bimodal powder mixtures prediction of sintered density for bimodal powder mixtures. Metall Mater Trans A 23A:1455–1465. https://doi.org/10.1007/BF02647329
19. Desmond KW, Weeks ER (2013) Influence of particle size distribution on random close packing of spheres. Phys Rev E 90:1–6
20. Aggarwal G, Park SJ, Smid I (2006) Development of niobium powder injection molding: Part I. Feedstock and injection molding. Int J Refract Met Hard Mater 24:253–262. https://doi.org/10.1016/j.ijrmhm.2005.06.003
21. Hidalgo J, Jiménez-Morales A, Torralba JM (2012) Torque rheology of zircon feedstocks for powder injection moulding. J Eur Ceram Soc 32:4063–4072. https://doi.org/10.1016/j.jeurceramsoc.2012.06.023
22. Amin A, Sri Yulis M, Muhamad N, Jamaludin KR, Abdullah S, Batu Pahat, P. (2007) Process, Rheological investigation of MIM feedstocks prepared with different particle sizes, in: World Eng Congr, Penang, Malaysia, 2007:212–218
23. Zakaria H, Muhamad N, Sulong AB, Irwan Ibrahim MH, Foudzi F (2014) Moldability characteristics of 3 mol% yttria stabilized zirconia feedstock for micro-powder injection molding process. Sains Malaysiana 43:129–136
24. Agote I, Odriozola A, Gutierrez M, Santamaría A, Quintanilla J, Coupelle P, Soares J (2001) Rheological study of waste porcelain feedstocks for injection moulding. J Eur Ceram Soc 21:2843–2853. https://doi.org/10.1016/S0955-2219(01)00210-2
25. Mohammad S, Ghasemi E, Alizadeh M, Yazdani R (2014) Processing research rheological properties of Mg based feedstocks with micro or nano Al2O3 powder for injection molding. J Ceram Process Res 15:236–241
26. Weir FE (1963) Moldability of plastics based on melt rheology. Part 1 - theoretical development. Polym Eng Sci 3:32–36. https://doi.org/10.1002/pen.760030108
27. Machaka R, Ndlangamandla P, Seerane M (2018) Capillary rheological studies of 17-4 PH MIM feedstocks prepared using a custom CSIR binder system. Powder Technol 326:37–43. https://doi.org/10.1016/j.powtec.2017.12.051
28. Oh JW, Lee WS, Park SJ (2018) Investigation and modeling of binder removal process in nano/micro bimodal powder injection molding. Int J Adv Manuf Technol 97:4115–4126. https://doi.org/10.1007/s00170-018-2263-8
29. Machaka R, Seerane M, Chikwanda HK, (2014) Binder development for metal injection moulding : a CSIR perspective
30. ASTM (2008) ASTM B962 - 08 Standard test methods for density of compacted or sintered powder metallurgy (PM) products using Archimedes' principle, ASTM B962 - 08 Stand. test methods density compact. or sintered powder Metall Prod Using Arch Princ
31. Spierings AB, Schneider M, Eggenberger R (2011) Comparison of density measurement techniques for additive manufactured metallic parts. Rapid Prototyp J 17:380–386. https://doi.org/10.1108/13552541111156504
32. Dihoru LV, Smith LN, Orban R, German RM (2000) Experimental study and neural network modeling of the stability of powder injection molding feedstocks. Mater Manuf Process 15:419–438
33. Suri P, Atre SV, German RM, de Souza JP (2003) Effect of mixing on the rheology and particle characteristics of tungsten-based powder injection molding feedstock. Mater Sci Eng A 356:337–344. https://doi.org/10.1016/S0921-5093(03)00146-1
34. Khakbiz M, Simchi A, Bagheri R (2005) Analysis of the rheological behavior and stability of 316L stainless steel–TiC powder injection molding feedstock. Mater Sci Eng A 407:105–113. https://doi.org/10.1016/j.msea.2005.06.057
35. Tatt TK, Muhamad N, Muchtar A, Sulong AB, Yunn HS (2012) Rheological behaviour of novel feedstock for manufacturing porous stainless steel via (MIM)-PSH. J Teknol (Sciences Eng) 59:187–191
36. Jamaludin KR, Muhamad N, Mohd MN, Ahmad S, Ibrahim MHI, Nor NHM (2009) Optimizing the injection parameter of water atomised SS316l powder with design of experiment method for best sintered density. Chiang Mai J Sci 36:349–358

37. Mohamad Nor N, Muhamad N, Ismail M, Jamaludin K, Ahmad S, Ibrahim M (2009) Flow behaviour to determine the defects of green part in metal injection molding. Int J Mech Mater Eng 4:70–75
38. German RM, Bose A (1997) Injection molding of metals and ceramics, 2nd edn. Metal Powder Industries Federation (Princeton, N.J., U.S.A), Princeton
39. Bose A, Otsuka I, Yoshida T, Toyoshima H (2008) Faster sintering and lower costs with ultra-fine MIM powders. Met Powder Rep 63: 25–30. https://doi.org/10.1016/S0026-0657(08)70058-4
40. Kearns M, Murray K, Tingskog T (2009) Effects of particle size and alloy chemistry on processing and properties of MIM powders BT - 2009 International Conference on Powder Metallurgy and Particulate Materials. PowderMet 2009:41–48
41. Todd I, Sidambe AT, 2013 Developments in metal injection moulding (MIM), in: Chang I, Zhao Y (Eds.), Adv Powder Metall Prop Process Appl, Woodhead Publishing, Sheffield, pp. 109–146. https://doi.org/10.1533/9780857098900.1.109
42. Muchavi NS, Bam L, de Beer FC, Chikosha S, Machaka R (2016) X-ray computed microtomography studies of MIM and DPR parts. J South Afr Inst Min Metall 116:973–980. https://doi.org/10.17159/2411-9717/2016/v116n10a13
43. Suri P, Smarslok BP, German RM (2006) Impact properties of sintered and wrought 17–4 PH stainless steel. Powder Metall 49: 40–47
44. Shi J, Cheng Z, Gelin JC, Barriere T, Liu B (2017) Sintering of 17-4PH stainless steel powder assisted by microwave and the gradient of mechanical properties in the sintered body. Int J Adv Manuf Technol 91:2895–2906. https://doi.org/10.1007/s00170-016-9960-y
45. Attia UM, Alcock JR (2011) A review of micro-powder injection moulding as a microfabrication technique. J Micromech Microeng 21:043001. https://doi.org/10.1088/0960-1317/21/4/043001
46. Murray K, Coleman AJ, Tingskog TA, Whychell DT Sr (2011) Effect of particle size distribution on processing and properties of MIM 17-4PH. Int J Powder Metall 47:21–28
47. Tang M, Pistorius PC (2017) Oxides , porosity and fatigue performance of AlSi10Mg parts produced by selective laser melting. Int J Fatigue 94:192–201. https://doi.org/10.1016/j.ijfatigue.2016.06.002
48. Fotovvati B, Namdari N, Dehghanghadikolaei A, (2019) Fatigue performance of selective laser melted Ti6Al4V components : state of the art, Mater Res Express 6
49. German RM (2018) MIM 17-4 PH stainless steel: processing, properties and best practice. Powder Inject Mould Int 12:49–76